Highly Accurate Electronic Structure of Metallic Solids from Coupled-Cluster Theory with Nonperturbative Triple Excitations

Verena A. Neufeld[1,2] and Timothy C. Berkelbach[1]
[1]*Department of Chemistry, Columbia University, New York, New York 10027, USA*
[2]*Division of Chemistry and Chemical Engineering, California Institute of Technology, Pasadena, California 91125, USA*

(Received 11 April 2023; accepted 28 September 2023; published 30 October 2023)

Coupled-cluster theory with single, double, and perturbative triple excitations (CCSD(T))—often considered the "gold standard" of main-group quantum chemistry—is inapplicable to three-dimensional metals due to an infrared divergence, preventing its application to many important problems in materials science. We study the full, nonperturbative inclusion of triple excitations (CCSDT) and propose a new, iterative method, which we call ring-CCSDT, that resums the essential triple excitations with the same N^7 run-time scaling as CCSD(T). CCSDT and ring-CCSDT are used to calculate the correlation energy of the uniform electron gas at metallic densities and the structural properties of solid lithium. Inclusion of connected triple excitations is shown to be essential to achieving high accuracy. We also investigate semiempirical CC methods based on spin-component scaling and the distinguishable cluster approximation and find that they enhance the accuracy of their parent *ab initio* methods.

DOI: 10.1103/PhysRevLett.131.186402

Introduction.—Accurately predicting energetic properties of metallic solids is crucial in computational materials science, with applications in heterogeneous catalysis, electrochemistry, and battery science [1–3]. Coupled-cluster theory with single and double excitations (CCSD) [4,5] has recently been shown to provide reasonable energies for the uniform electron gas (UEG) [6–8] and for atomistic metallic solids, such as lithium and aluminum [9–12], but it does not reliably outperform density functional theory (DFT), which is significantly cheaper—some inclusion of connected triple excitations is clearly required. For nonmetallic main-group solids, CCSD with perturbative triple excitations [CCSD(T)] [13] is highly accurate for bulk properties [14–18] and surface chemistry [18–24], mirroring its performance on molecules, where it commonly yields "chemical accuracy" of about 1 kcal/mol [5]. However, CCSD(T) is not expected to be applicable to three-dimensional metals: an approximate evaluation of the CCSD(T) energy of the UEG was shown to diverge in the thermodynamic limit [25], similar to the textbook result of second-order perturbation theory [26,27].

Here, we investigate the accuracy of CC theory with nonperturbative triple excitations (CCSDT) to determine whether such a theory provides the desired accuracy for metals. Because the high cost of CCSDT limits its routine application, we also design and test lower cost alternatives. Below, we first review diagrammatic results on the ground-state energy of the UEG, including its high-density expansion, divergences and necessary resummations, and connections with coupled-cluster theory including double and triple excitations. An analysis of the (T) correction for the UEG motivates a new theory, which nonperturbatively retains the triple excitations necessary to preclude a divergence and which has the same N^7 computational scaling as CCSD(T). We assess the performance of these methods with applications to the UEG at metallic densities and to solid lithium. Furthermore, we test several semiempirical modifications, including the distinguishable cluster (DC) approximation [28–30] and spin-component -scaled (SCS) CC theory [31–33], which were designed to approximate the effect of higher excitations without increasing the computational cost (we use the term "semiempirical" to indicate that, although in some cases the modifications can be constrained by physical principles, the methods are not rigorously diagrammatic).

Diagrammatic results on the uniform electron gas.—The UEG, a model of interacting electrons in a uniform positive background, has been a famous testing ground for new developments in nonperturbative many-body quantum field theory. Specifically, the total energy of the UEG with electron density n has been evaluated to leading orders in the Wigner-Seitz radius $r_s = [3/(4\pi n)]^{1/3}$ [27,34,35], in the absence and presence of a spin polarization; in this Letter, we focus on the upolarized case. The kinetic energy and Hartree-Fock (HF) exchange energy produce terms of $O(r_s^{-2})$ and $O(r_s^{-1})$, respectively, and the remaining terms define the correlation energy.

From dimensionality arguments, it is expected that second-order perturbation theory contributes all terms of $O(r_s^0)$, which is correct for the second-order exchange energy [27,36]. The second-order direct (ring) term, whose diagram is shown in Fig. 1(a), contributes a correlation energy $E_{2,4} \propto r_s^0 \int_0^\infty dq f(q)/q^2$, where

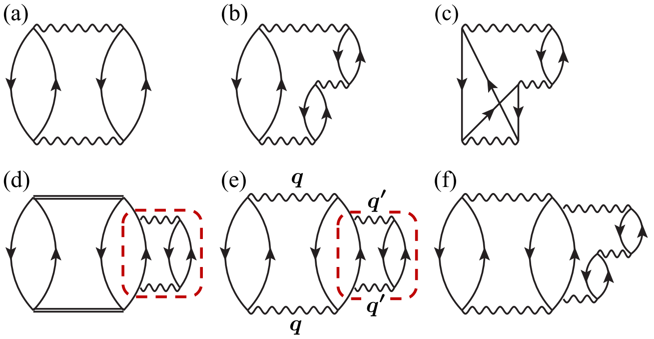

FIG. 1. Goldstone diagrams discussed in the text, which are included at various orders in perturbation theory and various flavors of CC theory. The dashed red box in (d) and (e) highlights the problematic feature responsible for the divergence of the CCSD(T) correlation energy.

$$f(q) = \int_{|\boldsymbol{k}+\boldsymbol{q}|>1} d^3k \int_{|\boldsymbol{p}+\boldsymbol{q}|>1} d^3p \frac{\theta(1-k)\theta(1-p)}{q^2 + (\boldsymbol{k}+\boldsymbol{p})\cdot\boldsymbol{q}} \qquad (1)$$

and all dimensionless momenta $\boldsymbol{k}, \boldsymbol{p}, \boldsymbol{q}$ are normalized to the Fermi momentum; we use the notation $E_{m,2n}$ from Refs. [34,35], where m is the order in perturbation theory and n is the number of interactions with the same momentum transfer. It can be shown that $f(q) \propto q$ in the limit $q \to 0$, and thus the second-order direct term famously diverges logarithmically. All higher order terms with the same ring structure (n rings at order n in perturbation theory), such as the one shown in Fig. 1(b) (i.e., $E_{3,6}$) exhibit the strongest divergences at each order, and their resummation to infinite order defines the random-phase approximation (RPA) [26,27,34,35,37–39], $\varepsilon' = E_{2,4} + E_{3,6} + E_{4,8} + \cdots$. The RPA provides a correlation energy that is correct to $O(\ln r_s)$ and is therefore exact in the high-density $r_s \to 0$ limit (aside from a constant); the appearance of terms $O(\ln r_s)$ in the density expansion signals the nonanalyticity of the correlation energy. As is well known, the CCSD energy contains all terms included in the RPA [40–42], providing a strong theoretical argument for the application of CC theories to metallic solids—a research agenda started more than 40 years ago [40,41,43,44]. As a reminder, single excitations vanish in the UEG by symmetry, and the CCSD correlation energy is $E_c = \frac{1}{4}\langle ij||ab\rangle t_{ij}^{ab}$, where t_{ij}^{ab} is the double-excitation amplitude that solves the CCSD amplitude equations. Here and henceforth, $i, j, \ldots$ indicate occupied spin orbitals, $a, b, \ldots$ indicate unoccupied spin orbitals, Coulomb integrals are in $\langle 12|12\rangle$ notation, the double bar indicates antisymmetrized integrals, and summation over repeated indices is implied.

Third-order perturbation theory produces convergent terms that are $O(r_s)$ (i.e., $E_{3,2}$), strongly divergent terms with three rings that are included in the RPA [i.e., Fig. 1(b) or $E_{3,6}$], and more weakly divergent terms whose diagrams have only one ring, such as that shown in Fig. 1(c), which define $E_{3,4}$. These latter terms have to be resummed with higher-order divergent contributions that have analogous structure ($n-2$ rings at order n in perturbation theory), $\varepsilon'' = E_{3,4} + E_{4,8} + \cdots$, which can be evaluated to identify a correlation energy that is exact to $O(r_s, r_s \ln r_s)$ [34,35,45]. Remarkably, all of these terms are included in the CCSD correlation energy. Although it has long been appreciated that CCSD resums the most divergent terms that define the RPA correlation energy ε' [40–42], to the best of our knowledge, it has not been noted that it also resums these next most divergent terms that define ε''. Therefore, CCSD is exact for the energy of the UEG to $O(r_s, r_s \ln r_s)$, which is one order higher than the RPA, in addition to recovering the correct constant term due to second-order exchange.

As expected, the CCSD energy is missing terms from fourth order in perturbation theory, including those that yield finite values of $O(r_s^2)$ or that diverge weakly and must be resummed with higher-order terms. CCSDT produces an energy that is exact to fourth order in perturbation theory and includes resummations necessary to eliminate fourth-order divergences, thus providing a potentially powerful theory of the energy of metals. However, CCSDT has a high computational cost that scales as N^8, which precludes routine application to atomistic materials. Nonetheless, below we exploit the simplicity of the UEG and carefully designed composite corrections to provide the first estimates of the performance of CCSDT for the UEG in the thermodynamic limit and for solid lithium.

The intermediate theory CCSD(T), with a reduced N^7 scaling, is very accurate for many molecules and insulating solids. However, CCSD(T) yields a divergent energy for metals, which was demonstrated numerically using an approximate form in Ref. [25]. Here, we provide a diagrammatic analysis of the same behavior to shed more light on the failures of CCSD(T). Neglecting single excitations, which vanish for the UEG by symmetry, the energy correction in CCSD(T) is shown by the diagram in Fig. 1(d) (plus permutations due to exchange), where the double line indicates t_{ij}^{ab} from CCSD. To lowest order, the (T) correction is that of bare fourth-order perturbation theory, shown in Fig. 1(e), whose analysis elucidates the (T) divergence. Considering only the contribution without exchange, the problematic process has four interactions with two pairs of identical momenta exchanged, $\boldsymbol{q}$ and $\boldsymbol{q}'$, i.e., the correlation energy is $E_c \propto r_s^2 \int d^3q \int d^3q' f(\boldsymbol{q},\boldsymbol{q}')/(q^4 q'^4)$, where

$$f(\boldsymbol{q},\boldsymbol{q}') = \int_{|\boldsymbol{k}+\boldsymbol{q}|>1} d^3k \int_{|\boldsymbol{m}+\boldsymbol{q}'|>1} d^3m \int_{\substack{|\boldsymbol{p}+\boldsymbol{q}|>1 \\ |\boldsymbol{p}-\boldsymbol{q}'|<1}} d^3p \frac{\theta(1-k)\theta(1-p)\theta(1-m)}{[q^2 + (\boldsymbol{k}+\boldsymbol{p})\cdot\boldsymbol{q}]^2 [q^2 + (\boldsymbol{k}+\boldsymbol{p})\cdot\boldsymbol{q} + (\boldsymbol{m}+\boldsymbol{p})\cdot\boldsymbol{q}']}. \qquad (2)$$

As usual, the correlation energy integral diverges due to the behavior of the integrand near $q, q' = 0$. Letting q_c be an infrared cutoff on both momentum integrals, the integrated result can be checked to diverge as $O(q_c^{-2} \ln q_c)$, demanding resummation with higher-order terms.

By replacing the outer Coulomb interactions by t_{ij}^{ab} from CCSD as in Fig. 1(d), CCSD(T) regularizes the integral over $\boldsymbol{q}$, but not $\boldsymbol{q}'$. This single ring diagram self-energy insertion, highlighted with a red box in Figs. 1(d) and 1(e), is responsible for the divergence of the CCSD(T) energy for metals. By analytically performing this regularization, the CCSD(T) energy can be shown to diverge as $O(\ln q_c)$, which is naturally weaker than that of bare fourth-order perturbation theory, but still useless for quantitative calculations. This rate of divergence is exactly the same as that of second-order perturbation theory, which we exploit in the Supplemental Material [46] to numerically confirm the divergence of CCSD(T), along the lines of other works [58,59].

Importantly, this analysis also identifies the minimal physics necessary to regularize the CCSD(T) approximation for metals, which is an infinite-order RPA-style resummation of ring diagrams in the self-energy insertion (like in the GW approximation [60]), as shown in Fig. 1(f). This can be achieved approximately by removing many of the terms from the CCSDT equations, analogous to the equivalence between (direct) ring-CCD and the RPA. This method, which we call ring-CCSDT, is implemented as follows. The singles and doubles amplitude equations are exactly as in CCSDT. The triples amplitude equation is the same as in the CCSDT-1 approximation [4,61–64], but is supplemented with direct ring diagrams, $0 = R_{\mathrm{CCSDT-1}} + R_{\mathrm{dr}}$,

$$\begin{aligned} R_{\mathrm{CCSDT-1}} = {} & \hat{P}(c/ab) f_{cd} t_{ijk}^{abd} - \hat{P}(k/ij) f_{lk} t_{ijl}^{abc} \\ & + \hat{P}(k/ij|a/bc)\langle bc||dk\rangle t_{ij}^{ad} \\ & - \hat{P}(i/jk|c/ab)\langle lc||jk\rangle t_{il}^{ab}, \end{aligned} \tag{3a}$$

$$\begin{aligned} R_{\mathrm{dr}} = {} & \hat{P}(i/jk|a/bc)\langle al|id\rangle t_{ljk}^{dbc} \\ & + \hat{P}(i/jk|abc)\langle lb|de\rangle t_{il}^{ad} t_{jk}^{ec} \\ & - \hat{P}(ijk|a/bc)\langle lm|dj\rangle t_{il}^{ad} t_{mk}^{bc} \\ & + \hat{P}(i/jk|a/bc)\langle lm|de\rangle t_{il}^{ad} t_{mjk}^{ebc}, \end{aligned} \tag{3b}$$

where $\hat{P}(k/ij|a/bc) = [1 - \hat{P}(ik) - \hat{P}(jk)][1 - \hat{P}(ab) - \hat{P}(ac)]$, $\hat{P}(ij)$ generates the permutation of i and j, and f_{pq} is a Fock matrix element. Note that Coulomb integrals in Eq. (3a) are antisymmetrized, whereas those in Eq. (3b) are not.

Unfortunately, despite its iterative nature, the CCSDT-1 approximation (without the ring diagrams) is a divergent theory of metals, like CCSD(T), because of the isolated ring diagram highlighted in Figs. 1(d) and 1(e). In the ring-CCSDT approximation, not all time orderings of repeated ring diagrams are included: all forward (Tamm-Dancoff) time orderings are included, which is sufficient to preclude a divergence [40], and a subset of the non-Tamm-Dancoff time orderings are included, but not all those corresponding to the complete RPA; this is very similar to the diagrammatic content of the coupled-cluster Green's function [65,66]. To include all time orderings that define RPA screening would require inclusion of connected quadruple excitations.

The first and last terms of R_{dr} exhibit N^8 computational scaling, like the parent CCSDT method. However, the use of direct (nonantisymmetrized) ring diagrams enables a reduction in scaling with the use of density fitting or Cholesky decomposition of the Coulomb integrals [67] $\langle pq||rs\rangle = \sum_P L_{pr}^P L_{qs}^P$, where P is an auxiliary index. For example, the last term can be constructed as

$$\sum_{lmde} \langle lm|de\rangle t_{il}^{ad} t_{mjk}^{ebc} = \sum_P \left[\sum_{ld} L_{ld}^P t_{il}^{ad}\right]\left[\sum_{me} L_{me}^P t_{mjk}^{ebc}\right]. \tag{4}$$

With such a compression of the Coulomb integrals, ring-CCSDT is an iterative N^7 method, providing an appealing alternative to the CCSD(T) approximation that is applicable to metals (although the storage of the triple excitation amplitudes t_{ijk}^{abc} is a separate bottleneck).

Results for the UEG.—CC approximations are difficult to treat semianalytically, even for the UEG. Therefore, we simulate a UEG of electron density n via a cubic box of N electrons with volume $V = N/n = (4/3)\pi r_s^3 N$ and a plane-wave orbital basis. Several correlated methods, especially CC and quantum Monte Carlo (QMC), have been previously applied to UEG models containing a finite number of electrons [68–71]; these models have a gap in their single-particle spectrum and thus do not suffer from the infrared divergences that arise in the TDL. However, study of these models enables direct comparison between different levels of theory and can also be viewed as a proxy for performance on other gapped systems such as molecules or insulating solids. In Table I, we present the correlation energy for $N = 14$, 54, and 114 at $r_s = 2$; to allow direct comparison, all results are at or near the complete basis set limit and are obtained without twisted boundary conditions. Overall, we see that CCSDT and DCSDT agree with each other and with QMC results to 0.5 mE_h or better. The new method ring-CCSDT is a significant improvement over CCSD, and achieves sub-$\mathrm{m}E_h$ accuracy compared to these latter reference methods. A more thorough comparison at $r_s = 0.5$, 1, 2, and 5 is given in the Supplemental Material [46].

Although the accuracy of various CC methods can be gleaned from these calculations with finite N, in this Letter we are primarily concerned with the critical question of their performance in the $N \to \infty$ limit. Specifically, we perform CCSD and DCSD calculations on systems containing up to $N = 1404$ electrons and estimate the complete basis set limit using calculations on smaller system sizes. These results are then used to extrapolate to the

TABLE I. UEG correlation energy per electron for $r_s = 2$ from various correlated methods at or near the complete basis set limit for $N = 14$, 54, and 114 electrons with a Γ-Point centered mesh. The first seven rows of data are from this Letter.

	E_c/N (mE_h)		
	$N = 14$	$N = 54$	$N = 114$
CCSD	−29.2	−30.2	−36.5
ring-CCSDT	−30.9	−32.3	−39.8
CCSDT	−31.4	−32.9	−40.7
SCS-CCSD	−36.2	−37.3	−44.9
DCSD	−30.5	−31.5	−38.9
SCS-DCSD	−32.6	−33.9	−41.9
DCSDT	−31.5	−33.0	−41.1
CCSDTQ [68]	−31.7	…	…
ph-AFQMC [72]	−31.6	−33.1	−40.7
DMC [69,73]	−31.0	−31.9	…
FCIQMC [74]	−31.8	…	…

thermodynamic limit assuming that finite-size errors in the correlation energy decay asymptotically as $N^{-2/3}$—a functional form that is derived in the Supplemental Material [46] and has also been proposed in recent work [75]. Our final CCSD correlation energies agree within about 1 mE_h with previous studies that targeted the thermodynamic limit [6,7], despite different technical details, providing a validation of our methods. CCSDT, ring-CCSDT, and DCSDT calculations are performed on systems containing up to $N = 156$ electrons, and we calculate the energy difference with respect to DCSD. The complete basis set limit of this energy difference is estimated based on smaller values of N and then extrapolated to the thermodynamic limit. Additional technical details are given in the Supplemental Material [46].

In Fig. 2, we present the correlation energy of the UEG at metallic densities of $r_s = 1$–5 from various CC theories as a fraction of the numerically exact result, estimated via recent Slater-Jastrow-backflow diffusion Monte Carlo (DMC) results [76]; a table of all values is given in the Supplemental Material [46]. The magnitude of the DMC correlation energy ranges from 60 mE_h at $r_s = 1$ to 29 mE_h at $r_s = 5$. As expected based on the density expansion discussed above, the relative accuracy of diagrammatic methods shown in Fig. 2(a) (CCSD, CCSDT, and ring-CCSDT) decreases with increasing r_s. Compared to CCSD, which recovers only about 76%–92% of the DMC correlation energy, CCSDT performs extremely well and recovers between 98% (at $r_s = 1$) and 92% (at $r_s = 5$), corresponding to an absolute accuracy of 1.3–2.4 mE_h. The good performance of ring-CCSDT, with errors of 1.7–3.2 mE_h, shows that the same ring diagram resummation responsible for curing the divergence of CCSD(T) is also responsible for most of the correlation energy associated with connected triple excitations.

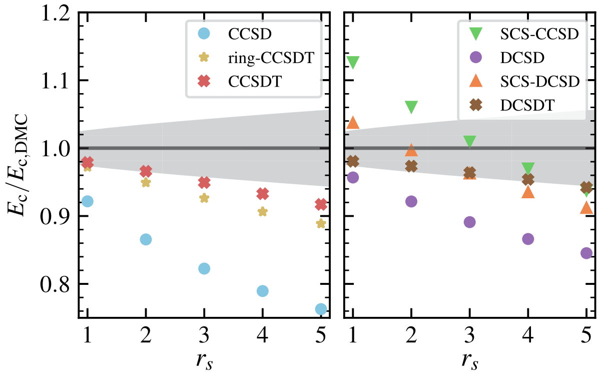

FIG. 2. Ratio of the coupled-cluster correlation energy to the diffusion Monte Carlo (DMC) correlation energy [76] for the three-dimensional UEG with $r_s = 1$–5, as given by the methods indicated in the legend. The methods are separated into those that are purely diagrammatic (left) and those that are semiempirical (right). Range of chemical accuracy (±1 kcal/mol or ±1.6 mE_h) is shown with a gray shaded area.

The semiempirical CC methods shown in Fig. 2(b) (SCS-CCSD, DCSD, SCS-DCSD, and DCSDT) typically perform better than their parent diagrammatic method. SCS-CCSD [32] improves over CCSD, except at small r_s, demonstrating that semiempirical modifications can spoil valuable formal properties like the exactness of CC theories in the high-density limit. DCSD [28] is better behaved and roughly halves the error of CCSD over this density range. SCS-DCSD [33] is a further improvement and provides the best overall performance of the N^6 scaling methods. Remarkably, DCSDT [29,30] yields results of extremely high accuracy, recovering more than 94% of the DMC correlation energy at all densities, which corresponds to an error of less than 1.7 mE_h, i.e., about 1 kcal/mol.

Results on solid lithium.—Next, we investigate the transferability of the above performance to a real material. We study solid lithium, which is a simple metal with a valence electron density corresponding to $r_s \approx 3.2$. We use CCSD, DSCD, ring-CCSDT, CCSDT, and DCSDT to calculate the equilibrium lattice parameter, bulk modulus, and cohesive energy. All calculations were performed with a development branch of PySCF [77–79], and all technical details—such as pseudopotentials, basis sets (up to quadruple-zeta Gaussian type orbitals), and Brillouin zone samplings (up to 64 k points, plus extrapolation)—are the same as in our previous work [11]; in that work, we found that CCSD predictions had significant room for improvement (at the CCSD level, we find that our updated finite-size extrapolations cause only small differences from our previous work, e.g., under 0.1 mE_h in the cohesive energy and under 0.01 Å for the lattice parameter). We estimate the ring-CCSDT, CCSDT, and DCSDT energies using composite corrections, by again considering the differences to DCSD, based on calculations with small

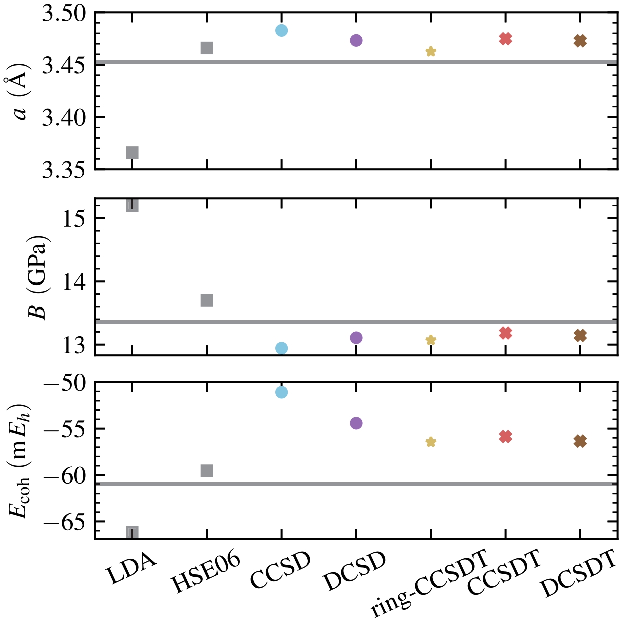

FIG. 3. Equilibrium lattice constant a, bulk modulus B, and cohesive energy E_{coh} for solid lithium. Results are shown at the indicated levels of CC theory and compared to experimental results [80–83] (solid horizontal lines), which have been corrected for zero-point vibrational energy using the HSE06 corrections from Ref. [80]. DFT results for the LDA and HSE06 functionals are shown for comparison (from Ref. [80]).

supercells (containing 8 and 16 Li atoms), frozen core orbitals, and frozen virtual natural orbitals [46].

Results are presented in Fig. 3, where they are compared to low temperature experimental results [80–83] that have been corrected for zero-point vibrational effects based on HSE06 phonon calculations [80]; a table of all values is given in the Supplemental Material [46]. Consistent with our results on the UEG, we see relatively systematic improvement with increasing sophistication of the theory. DCSD, ring-CCSDT, CCSDT, and DCSDT are all improvements over CCSD and they achieve accuracies of 0.009–0.022 Å, 0.16–0.28 GPa, and 4.5–6.6 mE_h in the lattice constant, bulk modulus, and cohesive energy, respectively. It is hard to disentangle the remaining discrepancies, which likely include some combination of pseudopotential, basis set, and finite-size error, incomplete correlation, and experimental uncertainty, including vibrational corrections. We also compare to DFT results reported in Ref. [80] using the LDA [84] and HSE06 [85–87] functionals. While the LDA functional does not predict accurate structural properties (despite its exactness for the UEG), the HSE06 functional performs very well. Importantly, we see that the improved methods explored in this Letter clearly outperform CCSD, bringing CC theory in line with the best performing DFT functionals.

Conclusion.—Despite the apparent simplicity of simple metals, including the UEG, achieving high accuracy for the electron correlation energy with *ab initio* wave function or diagrammatic methods is clearly a challenge. By contrast, this limit is almost trivial for DFT, where the LDA plus gradient corrections is ideal. We have shown that within the family of CC theories, the infinite-order inclusion of connected triple excitations is essential, although semiempirical treatments of these effects are surprisingly effective. We expect that the methods explored here, which have been evaluated for their ability to predict the properties of nearly uniform systems, will outperform DFT for more heterogeneous and complex systems, such as those arising in surface chemistry that require accurate treatments of dispersion interactions and stretched bonds. Before CC methods are widely used in this context, their comparatively high computational and storage costs must be addressed. However, in the meantime, they can be used to provide predictions of benchmark quality, especially in the many situations where experimental values cannot be obtained to the required precision.

Note added.—Recently, a related work by Masios *et al.* [88] appeared, proposing a new method that removes the infrared divergence from CCSD(T).

Data for this study can be found at [89].

We thank James Callahan and Xiao Wang for helpful discussions. This work was supported by the Columbia Center for Computational Electrochemistry and the National Science Foundation under Grant No. CHE-1848369. We acknowledge computing resources from Columbia University's Shared Research Computing Facility project, which is supported by NIH Research Facility Improvement Grant No. 1G20RR030893-01, and associated funds from the New York State Empire State Development, Division of Science Technology and Innovation (NYSTAR) Contract No. C090171, both awarded April 15, 2010. Data analysis and visualization were performed using NumPy [90], SciPy [91], PANDAS [92], MATPLOTLIB [93], SEABORN [94], and JaxoDraw [95]. UEG calculations used Julia [96], Fermi.jl [97], TensorOperations.jl [98], and Tullio.jl [99].

[1] J. K. Nørskov, F. Abild-Pedersen, F. Studt, and T. Bligaard, Density functional theory in surface chemistry and catalysis, Proc. Natl. Acad. Sci. U.S.A. **108**, 937 (2011).

[2] F. Calle-Vallejo and M. T. M. Koper, First-principles computational electrochemistry: Achievements and challenges, Electrochim. Acta **84**, 3 (2012).

[3] Q. He, B. Yu, Z. Li, and Y. Zhao, Density functional theory for battery materials, Energy Environ. Sci. **2**, 264 (2019).

[4] I. Shavitt and R. J. Bartlett, *Many-Body Methods in Chemistry and Physics: MBPT and Coupled-Cluster Theory*, Cambridge Molecular Science (Cambridge University Press, Cambridge, England, 2009), 10.1017/CBO9780511596834.

[5] R. J. Bartlett and M. Musiał, Coupled-cluster theory in quantum chemistry, Rev. Mod. Phys. **79**, 291 (2007).

[6] J. J. Shepherd, Communication: Convergence of many-body wave-function expansions using a plane-wave basis in the thermodynamic limit, J. Chem. Phys. **145**, 031104 (2016).

[7] T. N. Mihm, B. Yang, and J. J. Shepherd, Power laws used to extrapolate the coupled cluster correlation energy to the thermodynamic limit, J. Chem. Theory Comput. **17**, 2752 (2021).

[8] J. M. Callahan, M. F. Lange, and T. C. Berkelbach, Dynamical correlation energy of metals in large basis sets from downfolding and composite approaches, J. Chem. Phys. **154**, 211105 (2021).

[9] H. Stoll, B. Paulus, and P. Fulde, An incremental coupled-cluster approach to metallic lithium, Chem. Phys. Lett. **469**, 90 (2009).

[10] T. N. Mihm, T. Schäfer, S. K. Ramadugu, L. Weiler, A. Grüneis, and J. J. Shepherd, A shortcut to the thermodynamic limit for quantum many-body calculations of metals, Nat. Comput. Sci. **1**, 801 (2021).

[11] V. A. Neufeld, H.-Z. Ye, and T. C. Berkelbach, Ground-state properties of metallic solids from *ab initio* coupled-cluster theory, J. Phys. Chem. Lett. **13**, 7497 (2022).

[12] L. Weiler, T. N. Mihm, and J. J. Shepherd, Machine learning for a finite size correction in periodic coupled cluster theory calculations, J. Chem. Phys. **156**, 204109 (2022).

[13] K. Raghavachari, G. W. Trucks, J. A. Pople, and M. Head-Gordon, A fifth-order perturbation comparison of electron correlation theories, Chem. Phys. Lett. **157**, 479 (1989).

[14] P. Schwerdtfeger, B. Assadollahzadeh, and A. Hermann, Convergence of the Møller-Plesset perturbation series for the fcc lattices of neon and argon, Phys. Rev. B **82**, 205111 (2010).

[15] G. H. Booth, A. Grüneis, G. Kresse, and A. Alavi, Towards an exact description of electronic wavefunctions in real solids, Nature (London) **493**, 365 (2013).

[16] A. Grüneis, A coupled cluster and Møller-Plesset perturbation theory study of the pressure induced phase transition in the LiH crystal, J. Chem. Phys. **143**, 102817 (2015).

[17] T. Gruber, K. Liao, T. Tsatsoulis, F. Hummel, and A. Grüneis, Applying the coupled-cluster ansatz to solids and surfaces in the thermodynamic limit, Phys. Rev. X **8**, 021043 (2018).

[18] T. Gruber and A. Grüneis, *Ab initio* calculations of carbon and boron nitride allotropes and their structural phase transitions using periodic coupled cluster theory, Phys. Rev. B **98**, 134108 (2018).

[19] T. Tsatsoulis, F. Hummel, D. Usvyat, M. Schütz, G. H. Booth, S. S. Binnie, M. J. Gillan, D. Alfè, A. Michaelides, and A. Grüneis, A comparison between quantum chemistry and quantum Monte Carlo techniques for the adsorption of water on the (001) LiH surface, J. Chem. Phys. **146**, 204108 (2017).

[20] T. Tsatsoulis, S. Sakong, A. Groß, and A. Grüneis, Reaction energetics of hydrogen on Si(100) surface: A periodic many-electron theory study, J. Chem. Phys. **149**, 244105 (2018).

[21] J. G. Brandenburg, A. Zen, M. Fitzner, B. Ramberger, G. Kresse, T. Tsatsoulis, A. Grüneis, A. Michaelides, and D. Alfè, Physisorption of water on graphene: Subchemical accuracy from many-body electronic structure methods, J. Phys. Chem. Lett. **10**, 358 (2019).

[22] B. T. G. Lau, G. Knizia, and T. C. Berkelbach, Regional embedding enables high-level quantum chemistry for surface science, J. Phys. Chem. Lett. **12**, 1104 (2021).

[23] T. Schäfer, F. Libisch, G. Kresse, and A. Grüneis, Local embedding of coupled cluster theory into the random phase approximation using plane waves, J. Chem. Phys. **154**, 011101 (2021).

[24] T. Schäfer, A. Gallo, A. Irmler, F. Hummel, and A. Grüneis, Surface science using coupled cluster theory via local Wannier functions and in-RPA-embedding: The case of water on graphitic carbon nitride, J. Chem. Phys. **155**, 244103 (2021).

[25] J. J. Shepherd and A. Grüneis, Many-body quantum chemistry for the electron gas: Convergent perturbative theories, Phys. Rev. Lett. **110**, 226401 (2013).

[26] W. Macke, Über die Wechselwirkungen im Fermi-gas. Polarisationserscheinungen, correlationsenergie, elektronenkondensation, Z. Naturforsch. A **5**, 192 (1950).

[27] M. Gell-Mann and K. A. Brueckner, Correlation energy of an electron gas at high density, Phys. Rev. **106**, 364 (1957).

[28] D. Kats and F. R. Manby, Communication: The distinguishable cluster approximation, J. Chem. Phys. **139**, 021102 (2013).

[29] D. Kats and A. Köhn, On the distinguishable cluster approximation for triple excitations, J. Chem. Phys. **150**, 151101 (2019).

[30] V. Rishi and E. F. Valeev, Can the distinguishable cluster approximation be improved systematically by including connected triples?, J. Chem. Phys. **151**, 064102 (2019).

[31] S. Grimme, Improved second-order Møller–Plesset perturbation theory by separate scaling of parallel- and antiparallel-spin pair correlation energies, J. Chem. Phys. **118**, 9095 (2003).

[32] T. Takatani, E. G. Hohenstein, and C. D. Sherrill, Improvement of the coupled-cluster singles and doubles method via scaling same- and opposite-spin components of the double excitation correlation energy, J. Chem. Phys. **128**, 124111 (2008).

[33] D. Kats, Improving the distinguishable cluster results: Spin-component scaling, Mol. Phys. **116**, 1435 (2018).

[34] W. J. Carr and A. A. Maradudin, Ground-state energy of a high-density electron gas, Phys. Rev. **133**, A371 (1964).

[35] T. Endo, M. Horiuchi, Y. Takada, and H. Yasuhara, High-density expansion of correlation energy and its extrapolation to the metallic density region, Phys. Rev. B **59**, 7367 (1999).

[36] L. Onsager, L. Mittag, and M. J. Stephen, Integrals in the theory of electron correlations, Ann. Phys. (N.Y.) **473**, 71 (1966).

[37] D. Bohm and D. Pines, A collective description of electron interactions. I. Magnetic interactions, Phys. Rev. **82**, 625 (1951).

[38] D. Pines and D. Bohm, A collective description of electron interactions: II. Collective vs individual particle aspects of the interactions, Phys. Rev. **85**, 338 (1952).

[39] D. Bohm and D. Pines, A collective description of electron interactions: III. Coulomb interactions in a degenerate electron gas, Phys. Rev. **92**, 609 (1953).

[40] D. L. Freeman, Coupled-cluster expansion applied to the electron gas: Inclusion of ring and exchange effects, Phys. Rev. B **15**, 5512 (1977).

[41] R. F. Bishop and K. H. Lührmann, Electron correlations: I. Ground-state results in the high-density regime, Phys. Rev. B **17**, 3757 (1978).

[42] G. E. Scuseria, T. M. Henderson, and D. C. Sorensen, The ground state correlation energy of the random phase approximation from a ring coupled cluster doubles approach, J. Chem. Phys. **129**, 231101 (2008).

[43] R. F. Bishop and K. H. Lührmann, Electron correlations. II. Ground-state results at low and metallic densities, Phys. Rev. B **26**, 5523 (1982).

[44] K. Emrich and J. G. Zabolitzky, Electron correlations in the Bogoljubov coupled-cluster formalism, Phys. Rev. B **30**, 2049 (1984).

[45] D. F. DuBois, Electron interactions: Part II. Properties of a dense electron gas, Ann. Phys. (N.Y.) **8**, 24 (1959).

[46] See Supplemental Material at http://link.aps.org/supplemental/10.1103/PhysRevLett.131.186402 for technical details of all calculations and a discussion of finite-size errors in metals, including numerical demonstration of convergent and divergent behaviors of the considered theories. The Supplemental Materials also contains Refs. [47–57].

[47] A. Baldereschi, Mean-value point in the Brillouin zone, Phys. Rev. B **7**, 5212 (1973).

[48] S. Zhang and H. Krakauer, Quantum Monte Carlo method using phase-free random walks with slater determinants, Phys. Rev. Lett. **90**, 136401 (2003).

[49] G. H. Booth, A. J. W. Thom, and A. Alavi, Fermion Monte Carlo without fixed nodes: A game of life, death, and annihilation in Slater determinant space, J. Chem. Phys. **131**, 054106 (2009).

[50] A. J. W. Thom, Stochastic coupled cluster theory, Phys. Rev. Lett. **105**, 263004 (2010).

[51] G. Cassella, H. Sutterud, S. Azadi, N. D. Drummond, D. Pfau, J. S. Spencer, and W. M. C. Foulkes, Discovering quantum phase transitions with fermionic neural networks, Phys. Rev. Lett. **130**, 036401 (2023).

[52] H. Luo and A. Alavi, Combining the transcorrelated method with full configuration interaction quantum Monte Carlo: Application to the homogeneous electron gas, J. Chem. Theory Comput. **14**, 1403 (2018).

[53] J. J. Shepherd, G. Booth, A. Grüneis, and A. Alavi, Full configuration interaction perspective on the homogeneous electron gas, Phys. Rev. B **85**, 081103(R) (2012).

[54] G. F. Giuliani and G. Vignale, *Quantum Theory of the Electron Liquid*, 1st ed. (Cambridge University Press, Cambridge/New York, 2005).

[55] S. Chiesa, D. M. Ceperley, R. M. Martin, and M. Holzmann, Finite-size error in many-body simulations with long-range interactions, Phys. Rev. Lett. **97**, 076404 (2006).

[56] T. Helgaker, W. Klopper, H. Koch, and J. Noga, Basis-set convergence of correlated calculations on water, J. Chem. Phys. **106**, 9639 (1997).

[57] F. Birch, Finite elastic strain of cubic crystals, Phys. Rev. **71**, 809 (1947).

[58] J. J. Shepherd, T. M. Henderson, and G. E. Scuseria, Range-separated Brueckner coupled cluster doubles theory, Phys. Rev. Lett. **112**, 133002 (2014).

[59] J. J. Shepherd, T. M. Henderson, and G. E. Scuseria, Coupled cluster channels in the homogeneous electron gas, J. Chem. Phys. **140**, 124102 (2014).

[60] L. Hedin, New method for calculating the one-particle Green's function with application to the electron-gas problem, Phys. Rev. **139**, A796 (1965).

[61] Y. S. Lee and R. J. Bartlett, A study of Be_2 with many-body perturbation theory and a coupled-cluster method including triple excitations, J. Chem. Phys. **80**, 4371 (1984).

[62] Y. S. Lee, S. A. Kucharski, and R. J. Bartlett, A coupled cluster approach with triple excitations, J. Chem. Phys. **81**, 5906 (1984).

[63] M. Urban, J. Noga, S. J. Cole, and R. J. Bartlett, Towards a full CCSDT model for electron correlation, J. Chem. Phys. **83**, 4041 (1985).

[64] J. Noga, R. J. Bartlett, and M. Urban, Towards a full CCSDT model for electron correlation. CCSDT-n models, Chem. Phys. Lett. **134**, 126 (1987).

[65] M. F. Lange and T. C. Berkelbach, On the relation between equation-of-motion coupled-cluster theory and the GW approximation, J. Chem. Theory Comput. **14**, 4224 (2018).

[66] J. Tölle and G. K.-L. Chan, Exact relationships between the GW approximation and equation-of-motion coupled-cluster theories through the quasi-boson formalism, J. Chem. Phys. **158**, 124123 (2023).

[67] F. Weigend, M. Kattannek, and R. Ahlrichs, Approximated electron repulsion integrals: Cholesky decomposition versus resolution of the identity methods, J. Chem. Phys. **130**, 164106 (2009).

[68] V. A. Neufeld and A. J. W. Thom, A study of the dense uniform electron gas with high orders of coupled cluster, J. Chem. Phys. **147**, 194105 (2017).

[69] K. Liao, T. Schraivogel, H. Luo, D. Kats, and A. Alavi, Towards efficient and accurate *ab initio* solutions to periodic systems via transcorrelation and coupled cluster theory, Phys. Rev. Res. **3**, 033072 (2021).

[70] J. McClain, J. Lischner, T. Watson, D. A. Matthews, E. Ronca, S. G. Louie, T. C. Berkelbach, and G. K.-L. Chan, Spectral functions of the uniform electron gas via coupled-cluster theory and comparison to the G W and related approximations, Phys. Rev. B **93**, 235139 (2016).

[71] J. S. Spencer and A. J. W. Thom, Developments in stochastic coupled cluster theory: The initiator approximation and application to the uniform electron gas, J. Chem. Phys. **144**, 084108 (2016).

[72] J. Lee, F. D. Malone, and M. A. Morales, An auxiliary-Field quantum Monte Carlo perspective on the ground state of the dense uniform electron gas: An investigation with Hartree-Fock trial wavefunctions, J. Chem. Phys. **151**, 064122 (2019).

[73] P. López Ríos, A. Ma, N. D. Drummond, M. D. Towler, and R. J. Needs, Inhomogeneous backflow transformations in quantum Monte Carlo calculations, Phys. Rev. E **74**, 066701 (2006).

[74] J. J. Shepherd, G. H. Booth, and A. Alavi, Investigation of the full configuration interaction quantum Monte Carlo

method using homogeneous electron gas models, J. Chem. Phys. **136**, 244101 (2012).

[75] T. N. Mihm, L. Weiler, and J. J. Shepherd, How the exchange energy can affect the power laws used to extrapolate the coupled cluster correlation energy to the thermodynamic limit, J. Chem. Theory Comput. **19**, 1686 (2023).

[76] S. Azadi, N. D. Drummond, and S. M. Vinko, Correlation energy of the paramagnetic electron gas at the thermodynamic limit, Phys. Rev. B **107**, L121105 (2023).

[77] Q. Sun, Libcint: An efficient general integral library for Gaussian basis functions, J. Comput. Chem. **36**, 1664 (2015).

[78] Q. Sun, T. C. Berkelbach, N. S. Blunt, G. H. Booth, S. Guo, Z. Li, J. Liu, J. D. McClain, E. R. Sayfutyarova, S. Sharma, S. Wouters, and G. K.-L. Chan, PySCF: The Python-based simulations of chemistry framework, WIREs Comput. Mol. Sci. **8**, e1340 (2018).

[79] Q. Sun *et al.*, Recent developments in the PySCF program package, J. Chem. Phys. **153**, 024109 (2020).

[80] G.-X. Zhang, A. M. Reilly, A. Tkatchenko, and M. Scheffler, Performance of various density-functional approximations for cohesive properties of 64 bulk solids, New J. Phys. **20**, 063020 (2018).

[81] R. Berliner and S. A. Werner, Effect of stacking faults on diffraction: The structure of lithium metal, Phys. Rev. B **34**, 3586 (1986).

[82] R. A. Felice, J. Trivisonno, and D. E. Schuele, Temperature and pressure dependence of the single-crystal elastic constants of Li 6 and natural lithium, Phys. Rev. B **16**, 5173 (1977).

[83] C. Kittel, *Introduction to Solid State Physics*, 8th ed. (John Wiley & Sons, Inc., New York, 2005).

[84] W. Kohn and L. J. Sham, Self-consistent equations including exchange and correlation effects, Phys. Rev. **140**, A1133 (1965).

[85] J. Heyd, G. E. Scuseria, and M. Ernzerhof, Hybrid functionals based on a screened Coulomb potential, J. Chem. Phys. **118**, 8207 (2003).

[86] J. Heyd, G. E. Scuseria, and M. Ernzerhof, Erratum: "Hybrid functionals based on a screened Coulomb potential" [J. Chem. Phys. 118, 8207 (2003)], J. Chem. Phys. **124**, 219906(E) (2006).

[87] A. V. Krukau, O. A. Vydrov, A. F. Izmaylov, and G. E. Scuseria, Influence of the exchange screening parameter on the performance of screened hybrid functionals, J. Chem. Phys. **125**, 224106 (2006).

[88] N. Masios, A. Irmler, T. Schäfer, and A. Grüneis, preceding Letter, Averting the infrared catastrophe in the gold standard of quantum chemistry, Phys. Rev. Lett. **131**, 186401 (2023).

[89] https://github.com/verena-neufeld/2023_data_for_paper_cc_metallic.

[90] C. R. Harris *et al.*, Array programming with NumPy, Nature (London) **585**, 357 (2020).

[91] P. Virtanen *et al.* (SciPy1.0 Contributors), SciPy1.0: Fundamental algorithms for scientific computing in Python, Nat. Methods **17**, 261 (2020).

[92] W. McKinney, Data structures for statistical computing in python, in *Proceedings of the 8th Python in Science Conference*, edited by S. van der Walt and J. Millman (2009), pp. 55–61, https://conference.scipy.org/proceedings/scipy2010/mckinney.html.

[93] J. D. Hunter, MATPLOTLIB: A 2d graphics environment, Comput. Sci. Eng. **9**, 90 (2007).

[94] M. L. Waskom, SEABORN: Statistical data visualization, J. Open Source Softwaare **6**, 3021 (2021).

[95] D. Binosi and L. Theußl, JaxoDraw: A graphical user interface for drawing Feynman diagrams, Comput. Phys. Commun. **161**, 76 (2004).

[96] J. Bezanson, A. Edelman, S. Karpinski, and V. B. Shah, Julia: A fresh approach to numerical computing, SIAM Rev. **59**, 65 (2017).

[97] G. J. R. Aroeira, M. M. Davis, J. M. Turney, and H. F. Schaefer III, Fermi.jl: A modern design for quantum chemistry, J. Chem. Theory Comput. **18**, 677 (2022).

[98] TensorOperations.jl, https://github.com/Jutho/TensorOperations.jl, accessed 2023-02-13.

[99] Tullio.jl, https://github.com/mcabbott/Tullio.jl, accessed 2023-02-13.